Control of Two Wheel Mobile Manipulator on a Rough Terrain using Reaction Torque Observer Feedback

Received 6th March 2009; accepted 24th September 2009.

Pradeep Kumara W. Abeygunawardhana, Toshiyuki Murakami

Abstract:

The two-wheel *mobile manipulator has the potential to become an efficient industrial robot due to its mobility and dexterity. Moreover, it has expanded the operational area of the mobile manipulator due to its ability to work in a limited space. However, adaptability to unknown environments has still not been developed to date. Therefore, adaptation of the* two-wheel *mobile manipulator for unknown environments especially for rough/irregular terrain is discussed in this paper. Information about the environment, a key factor when aiming for compliance with an unknown and/or unstructured environment, was collected using a reaction torque observer. In order to adapt to the environment, compliance control was applied to the* two-wheel *mobile manipulator. In this paper, we present a novel control strategy we have developed that can deal with unknown environments through the effective use of inverted pendulum control. Simulation and experiments were carried out to ensure the validity of the proposed method. The method could be confirmed as effective according to the results obtained.*

Keywords: *two-wheel mobile manipulator, inverted pendulum control, environment interaction, reaction torqueo, compliance control.*

1. Introduction

Mobility in outdoor unstructured or semi-structured environments is an important consideration for mobile robotic systems. The intelligence for generating adaptive motor function is important when improving mobility under such an environment. This paper addresses the robot environment interaction of the two-wheel mobile manipulator using a reaction torque observer. We have developed adaptive motor functions of wheel motors for uneven floor surfaces for the two-wheel mobile manipulator.

Mobile manipulation provides the dual advantage of mobility and dexterity offered by the platform and the manipulator, respectively. The degree of freedom of the platform is also added the redundancy of the system. These systems can be effectively used for a variety of tasks such as industrial robots, service robotics etc. The two-wheel mobile manipulator has the ability to balance on its two-wheels and spin on the spot. This additional maneuverability allows easy navigation on various terrains, the turning of sharp corners and making of traverse small steps or curbs. The inverted pendulum problem is one of the common problems in the field of control engineering. The technology that has evolved from this unstable system is popular among researchers around the world [1],[2]. Consequently, it has been used to implement self-balanced robots by many research groups [3], [4],[5]. The two-wheel mobile manipulator is one of the most recent self-balanced robots in which inverted pendulum control has been used [6].

More recently stability improvements have been proposed using null space control [7] and control gain switching [8]. However, the two-wheel mobile manipulator is expected to work in a dynamic environment in industry. Therefore this robot should be intelligent enough to cope with an unknown or unstructured environment. This paper proposes an embedded motor function, which develops the affinity and adaptability of the two-wheel mobile manipulator to the environment. In a real environment, there are different kinds of agents such moving objects, immobile objects and rough surfaces. Detecting the environment is a critical issue in developing intelligent motor functions resistant to environmental disturbances. Researchers have utilized in the recent past different kinds of detection methods such as sonar sensors, cameras, sensors with additional memory functions and force sensors [9],[10],[11] etc. Even though many detection methods have been reported on, an enduring problem has been that it is not easy to get precise information about floor due to viscous friction and floor elasticity.

However, the reaction torque observer is a good candidate for obtaining this kind of environmental information [11]. Hence our choice to use the reaction torque observer to gather information on rough floors as described in this paper. Another advantage of this system is its low cost implementation due to being a sensor less application. The robot should be adapted to the environment and this adaptation can be implemented based on the remote and contact information collected. Trajectory tracking and obstacle avoidance derived from positional information are important considerations for adaptation by remote information. Among the significant applications, certain functions can be highlighted, namely: obstacle avoidance and robot navigation using potential functions [13],[14], obstacle avoidance control via sliding mode approach [15], near time optimal trajectory planning for wheeled mobile robots [16] and route planning for mobile robots amidst moving obstacles [17]. A versatile controller against environment change has been developed for a power assistant platform [18] and also a wheelchair robot [19] based on contact information. This paper uses the compliance control as a compensation method, which can smoothly compensate the environmental disturbances [20],[25]. Wheel and manipulator controllers are combined by means of a virtual

inverted pendulum model. Here, balancing of robot should be accomplished while achieving other motion targets. No research work has been reported to date reporting on the use of a reaction torque observer with inverted pendulum control. Therefore, this paper proposes an innovative embedded motor function, which can deal with the environment for the two-wheel mobile manipulator. In summary, this paper presents a control method that compensates the environment. Disturbances, which are detected through the reaction torque observer, do not affect the inverted pendulum control and trajectory control.

Fig. 1. Two-wheel vehicle.

This paper is presented in seven sections. Following this introduction section II describes the modeling of the robot. Section III explains the double inverted pendulum and section IV describes the development of a robust wheel controller. Section V presents the manipulator control and Section VI gives a brief introduction to the disturbance observer and the reaction torque observer. Section VII has been organized in two parts as the simulation and the experiment. Each parts gives test procedure, parameters and results. Finally, we close the paper with the conclusion.

2. Modeling

The model for the proposed device is described in this section. The two-wheel robot has a coaxial two-wheel system. A Direct Current (DC) servo motor with an encoder used to measure wheel angles has been mounted on one wheel. A vehicle body with three link manipulators and a wheel system are assembled together. Each manipulator link is controlled using a DC servo motor with encoder. The body is connected to the wheel system *via* a passive joint. The angle of the passive joint is measured using an inclination sensor. The body connected through the passive joint, is also assumed to be a manipulator link. Therefore, the robot has the form of a two-wheel robot with four degrees of freedom manipulator.

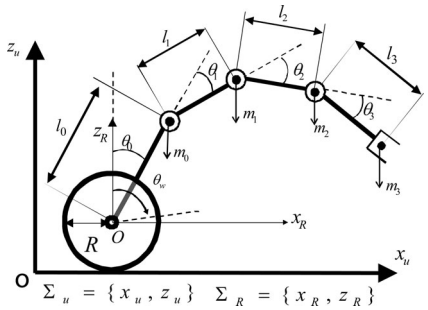

Fig. 2. Model of two-wheel mobile robot.

A. Dynamics

The dynamic modeling is described in this section. The model of the robot is shown in Fig. 2.

Variables of this model are given in Table 1.

Table 1. Dynamic model parameters.

θ_0	Inclination angle of the vehicle body
m_0	Mass of the vehicle body
θ_i	$i=1,2,3$ Joint angle of link i
m_i	$i=1,2,3$ Mass of link i
m_w	Mass of a wheel
θ_w	Rotation angle of wheels
l_0	Distance between wheel center and center of body
l_i	The length of the ith link
R	Radius of wheels
Σ_u	Universal coordinate
Σ_R	Robot coordinate

In this derivation, we have assumed that mass of a link is located at the top of the link. θ_0 is the angle of the passive joint and the manipulator works in X-Z plane. X axis is selected horizontally parallel to the floor and Z axis is selected vertically. x_R and z_R are the robot's coordinates. Clockwise rotation of the vehicle body, wheels and all links are positive. In this model, dynamic equations are formulated using the Lagrange equation of motion. The Lagrange equation is shown in (1).

$$\frac{d}{dt}\left(\frac{\partial L}{\partial \dot{q}_i}\right)-\frac{\partial L}{\partial q_i}=\tau_i, \quad i=1,2,...n \tag{1}$$

L is called Lagranrian function and is given by "$L = T - U$". Definitions of parameters are given by (Table 2).

Table 2. Dynamic model parameters.

L	Lagranrian function
T	Kinetic energy of the system
U	Potential Energy of the system
τ_i	External torques
θ_i	$i=w,0,1,2,3$ angles of wheel, passive joint and links $1,2,3$

Kinetic energy of this system is given by eq. (2)

$$T=\frac{1}{2}\left\{\left(m_w v_w^2+I_w\dot{\theta}_w^2\right)+\left(m_0 v_0^2+I_0\dot{\theta}_0^2\right)+\right. \tag{2}$$
$$\left.+\left(m_1 v_1^2+I_1\dot{\theta}_1^2\right)+\left(m_2 v_2^2+I_2\dot{\theta}_2^2\right)+\left(m_3 v_3^2+I_3\dot{\theta}_3^2\right)\right\}$$

$$U=g\left\{\left(m_w h_w\right)+\left(m_0 h_0\right)+\left(m_1 h_1\right)+\left(m_2 h_2\right)+\left(m_3 h_3\right)\right\} \tag{3}$$

where v denotes the linear velocity and h represents height from the wheel center to mass center of the link. I is the moment of inertia of the corresponding links. By simplifying (2) and (3) with (1), we can obtain dynamics of the system as (4).

$$\tau = M\ddot{\theta}+H+G \tag{4}$$

where, τ is the vector of motor torques. M is inertia matrix. H represents coriolis acceleration coefficient and centrifugal acceleration coefficient. G represents gravity.

B. Double inverted pendulum

Inverted pendulum having two stages is called double inverted pendulum. The stability margin of a double inverted pendulum is larger than that of a single inverted pendulum. The former is used in this paper and a model of it is shown in Fig. 3.

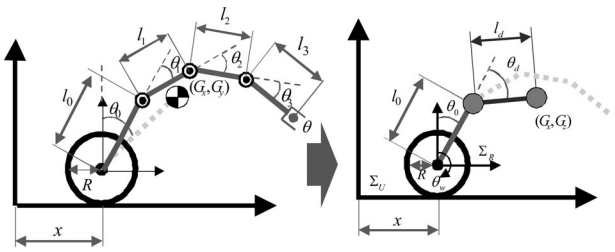

Fig. 3. Double inverted pendulum model.

G_x x position of COG (Center Of Gravity)
G_z z position of COG
l_d Length of second pendulum
θ_d Angle of second pendulum

In our system, we have three link manipulators and the robot body. Therefore the manipulator system has four degrees of freedom. Equivalent mass center and its position for the input into the manipulator system can be calculated for this system as (5) and (6). At this point we have a virtual robot body and an inverted pendulum. Ultimately it becomes a virtual double inverted pendulum system [6]. We used abbreviations to express equations (5) and (6) and those are given in (7).

$$G_x = \frac{m_1 l_0 S_0 + m_2 l_1 S_{01} + m_3 l_2 S_{012} + m_4 l_3 S_{0123}}{m_0 + m_1 + m_2 + m_3} \tag{5}$$

$$G_z = \frac{m_1 l_0 C_0 + m_2 l_1 C_{01} + m_3 l_2 C_{012} + m_4 l_3 C_{0123}}{m_0 + m_1 + m_2 + m_3} \tag{6}$$

$$\begin{cases} S_0 = \sin\theta_0 \\ C_0 = \cos\theta_0 \\ S_{01} = \sin(\theta_0 + \theta_1) \\ C_{01} = \cos(\theta_0 + \theta_1) \\ S_{012} = \sin(\theta_0 + \theta_1 + \theta_2) \\ C_{012} = \cos(\theta_0 + \theta_1 + \theta_2) \\ S_{0123} = \sin(\theta_0 + \theta_1 + \theta_2 + \theta_3) \\ C_{0123} = \cos(\theta_0 + \theta_1 + \theta_2 + \theta_3) \end{cases} \tag{7}$$

The length of the second pendulum and the angle of the second pendulum are given by equations (8) and (9).

$$l_d = \sqrt{(G_x - l_0 S_0)^2 + (G_z - l_0 C_0)^2} \tag{8}$$

$$\theta_d = \sin^{-1}\left(\frac{G_x - l_0 S_0}{l_0}\right) - \theta_0 \tag{9}$$

A dynamic equation of the double inverted pendulum is derived by using equation (1) and is given as shown in (10).

$$\tau_d = M_d(q)\ddot{q} + h_d(q,\dot{q}) + g_d(q) \tag{10}$$

Where, $q = [x, \theta_0, \theta_d]^T$, $\tau = [F, 0, 0]^T$
$M_d(q)$ is a 3 x 3 symmetric matrix and components are given in (III). Matrices $h_d(q,\dot{q})$ and $g_d(q)$ are given by equations (11) and (12).

$$h_d = \begin{bmatrix} -(m_0 + M_1) l_0 \sin\theta_0 . \dot{\theta}_0^2 - M_1 l_d \sin\theta_d . \dot{\theta}_d^2 \\ M_1 l_0 l_d \sin(\theta_0 - \theta_d)\dot{\theta}_0\dot{\theta}_d \\ M_1 l_0 l_d \sin(\theta_0 - \theta_d)\dot{\theta}_0^2 \end{bmatrix} \tag{11}$$

$$g_d = \begin{bmatrix} 0 \\ (m_0 + M_1) g l_0 \sin\theta_0 \\ M_1 g l_d \sin\theta_0 \end{bmatrix} \tag{12}$$

Table 3. Elements $M_d(q)$.

$m_{d11} = (m_w + m_0 + M_2)$	$m_{d12} = (m_0 + M_1) l_0 cos\theta_0$
$m_{d13} = M_1 l_d cos\theta_d$	$m_{d21} = (m_0 + M_1) l_0 cos\theta_0$
$m_{d22} = (m_0 + M_1) l_0^2$	$m_{d23} = M_1 l_0 l_d cos\theta_d(\theta_0 - \theta_d)$
$m_{d31} = M_1 l_d cos\theta_d$	$m_{d32} = M_1 l_0 l_d cos\theta_d(\theta_0 - \theta_d)$
$m_{d33} = M_1 l_d^2$	

Here m_w is the mass of wheels m_0 is the mass of Body and M_1 is the mass of the second pendulum and it is calculated as $M_1 = m_1 + m_2 + m_3$. The dynamics of the double inverted pendulum are given in matrix form as explained by (10)-(12). Assuming that the passive joint angle, θ_0 and the angle of the second pendulum, θ_d are small angles, we simplify the second equation of (10). Since l_0 is not equal to zero, (13) was obtained. The relationship between the linear acceleration and the angular acceleration of wheels is shown as (14). Stabilization control of the two-wheeled mobile manipulator was implemented using (13) and (14).

$$\ddot{\theta}_0 = -\frac{1}{l_0}\left(\ddot{x} + \frac{M_2 l_d \ddot{\theta}_d}{M_1 + M_2} + g\theta_0\right) \tag{13}$$

$$\ddot{x} = R\ddot{\theta}_w \tag{14}$$

In our system, θ_0 which does not have a control input is the angle of passive joint. In order to stabilize the whole system, it is necessary to control θ_0. The only way that θ_0 can be controlled, is to control the wheel acceleration. Hence, the control equation (15) is approximated.

$$\ddot{\theta}_w = K_{pd}(\theta_0^{res} - \theta_0^{cmd}) + K_{vd}(\dot{\theta}_0^{res} - \dot{\theta}_0^{cmd}) - \frac{M_1 l_d \ddot{\theta}_d}{(m_0 + M_1)R} \tag{15}$$

K_{pd} is the position gain of wheel command estimation and K_{vd} is the velocity gain of wheel command estimation. θ_0^{res} and $\dot{\theta}_0^{res}$ are angle and angular velocity of robot

body or passive joint, which are, measured a using gyro sensor. θ_0^{cmd} and $\dot{\theta}_0^{cmd}$ are command values and equal to zero.

$\frac{M_1 l_d \ddot{\theta}_d}{(m_0 + M_1)R}$ is the interactive effect of the second pendulum. Equation (15) was substituted with (13) and (14) combined and a Laplace transformation was performed for resultant equation. Finally, G(s) can be obtained.

$$G(s) = \frac{\theta_0^{res}}{\theta_0^{cmd}} = \frac{\frac{R}{l_0}\left(K_{pd} + K_{vd}s\right)}{s^2 + \frac{R}{l_0}K_{vd}s + \frac{1}{l_0}\left(RK_{pd} + g\right)} \tag{16}$$

$$\omega_n = \sqrt{\frac{1}{l_0}\left(RK_{pd} + g\right)} \qquad \zeta = \frac{K_{vd}R}{2l_0\omega_n} \tag{17}$$

This is a second order transfer function. Natural angular frequency, ω_n and damping coefficient, ζ are given in (17). K_{pd} and K_{vd} were selected such that the system is stable. To realize the wheel control, the angular acceleration of wheel, $\ddot{\theta}_w$, which was estimated as described in (15) was taken as an acceleration command to the wheel motors. Then, estimated angular position and angular velocity are generated by integrating the angular acceleration command. The calculation process is represented by (18). Finally, estimated angular position and angular velocity are taken as angular position command, θ_w^{cmd} and angular velocity command, $\dot{\theta}_w^{cmd}$ to the wheel motor as described in (19).

$$\dot{\theta}_w = \int \ddot{\theta}_w dt, \quad \theta_w = \int \dot{\theta}_w dt \tag{18}$$

$$\ddot{\theta}_w^{cmd} = \ddot{\theta}_w, \quad \dot{\theta}_w^{cmd} = \dot{\theta}_w, \quad \theta_w^{cmd} = \theta_w \tag{19}$$

3. Development of robust wheel controller using compliance control

In rough terrain, there may be some steps and random items such as pieces of stone. When the robot collapses due to such an item, it is because there have been forces acting on the wheels of the robot. The controller should have been robust enough to handle these forces. In this section we explain the implementation of a robust controller for rough terrain. List of symbols that we used in this section is given by Table 4.

Table 4. Wheel controller parameter.

x_v^{cmd}	Linear position command of the wheel
$\dot{x}_v^{cmd}$	Linear velocity command of the wheel
x_v^{res}	Linear position response of the wheel
$\dot{x}_v^{res}$	Linear velocity response of the wheel
F_{env}	Force from the environment
$\hat{\tau}_{reac}$	Estimated reaction torque
$\ddot{x}_{env}$	Estimated acceleration of the environment
$\dot{x}_{env}$	Estimated velocity of the environment
x_{env}	Estimated position of the environment
K_p	Position gain of wheel controller
K_v	Velocity gain of wheel controller

Obviously, the wheel controller is basically a simple Proportional and Derivative (PD) controller. Angular velocity command, θ_w^{cmd} and angular position command of wheel, $\dot{\theta}_w^{cmd}$ were reckoned using the double inverted pendulum model as described in the previous section. These angular commands can be converted into linear commands as shown in (20) and (21). Hence, the acceleration reference of the wheel was drawn as described by (22). K_p and K_v are proportional gain and velocity gain of wheel controller.

$$\dot{x}_v^{cmd} = R\dot{\theta}_v^{cmd} \tag{20}$$

$$x_v^{cmd} = R\theta_v^{cmd} \tag{21}$$

$$\ddot{x}_v^{ref} = K_p(x_v^{cmd} - x_v^{res}) + K_v(\dot{x}_v^{cmd} - \dot{x}_v^{res}) \tag{22}$$

This simple controller was modified by including a compliance control. Reaction torque estimated through the reaction torque observer is used for compliance control. Fig. 4 illustrates the translational and rotational direction force components. In this approach the force component in the rotational direction is zero.

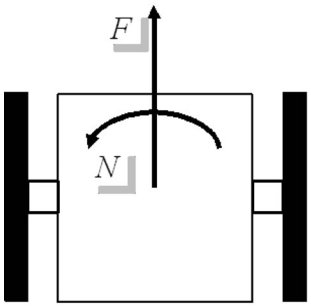

Fig. 4. Translational and rotational force component of the robot.

When the wheels of the robot collide with some object on the floor, it produces forces back on wheels. These forces are estimated by reaction torque observers implemented on wheel motors as torques. These reaction torques are transformed into the translational direction as explained in (23).

$$F_{env} = \frac{1}{R}\tau_{reac} \tag{23}$$

Estimated forces are converted into position characteristics using compliance control. If the virtual impedance characteristics of the environment are M_{env}, D_{env} and K_{env}, the conversion of reaction force into the position command is shown in (24). Aenv is feedback gain of external force.

$$M_{env}\ddot{x}_{env} + D_{env}\dot{x}_{env} + K_{env}x_{env} = A_{env}F_{env} \tag{24}$$

Using (24), it is possible to calculate the position feedback and velocity feedback from the environment. The acceleration reference command to the wheel motor is modified as shown in (25).

$$\begin{aligned}\ddot{x}_v^{ref} &= K_p(x_v^{cmd} - x_v^{res} - x_{env}) + \\ &+ K_v(\dot{x}_v^{cmd} - \dot{x}_v^{res} - \dot{x}_{env}) - \ddot{x}_{env}\end{aligned} \tag{25}$$

Final acceleration reference value to the wheel motor is implemented as in (25). An acceleration command is produced by the robust control system based on the disturbance observer and is transformed into torque by motor inertia. Here, if only the ingredient of one degree of freedom is taken out and the

Laplace conversion is carried out, it yields,

$$x_v^{res} = \frac{K_p + K_v s}{s^2 + K_v s + K_p} x_v^{cmd} - \frac{\frac{K_{env}}{M_{env}}}{s^2 + \frac{D_{env}}{M_{env}} s + \frac{K_{env}}{M_{env}}} \frac{A_{env}}{K_{env}} F_{env} \quad (26)$$

$$x_v^{res} = \frac{2\zeta_p \omega_p s + \omega_p^2}{s^2 + 2\zeta_p \omega_p s + \omega_p^2} x_v^{cmd} - \\ - \frac{\omega_{env}^2}{s^2 + 2\zeta_{env} \omega_{env} s + \omega_{env}^2} C_{env} F_{env} \quad (27)$$

Where,

ζ_p, ω_p - Position response characteristics with respect to position command x_v^{cmd},

ζ_{env}, ω_{env} - Position response characteristics with respect to environment force F_{env},

C_{env}, - Compliance characteristics.

By this method, separate designs of characteristics for each input (x_v^{cmd}, F_{env}) can be obtained. It is possible to attain the desired compliance characteristic C_{env}, maintaining performance of its position control.

Fig. 5 shows a block diagram of the wheel controller. The control strategy has already been elaborated on; describing how a velocity reference is generated to the wheel motor. The robot presented in this paper is commanded through a pendulum model. A virtual double inverted pendulum model was constructed utilizing manipulator dynamics and wheel dynamics. Acceleration commands to the wheel are generated using inverted pendulum control so that the body can maintain its balanced position. Desired body angle (θ_0^{cmd}) is determined by the pendulum model according to the commanded COG position. The inclination sensor that was mounted on the robot body is used to measure the actual angle of the body (θ_0^{res}). With the help of this data, an acceleration command is derived and elaborated inside the pendulum controller in Fig. 5 and this process was explained by section 2B.

The angular acceleration command is converted into linear mode. Velocity and position commands for the wheel motor are calculated by integrating the linear acceleration command. A reference motor current is calculated using motor inertia, gear ratio and current constant. A disturbance observer compensates the disturbances of the wheel motor. Reaction torque feedback is used to modify the trajectory in such a way that the robot can adapt to the changing environment. Reaction torque observers are implemented for each wheel motor and the outputs of those are taken as the input to the compliance controller. The strategy that was used to modify the wheel PD controller is depicted in Fig. 5 as a compliance controller.

4. Posture control of manipulator using cog control

Kinematic relationship can be expressed as shown in (28)-(30). q is the joint angle vector and is defined by

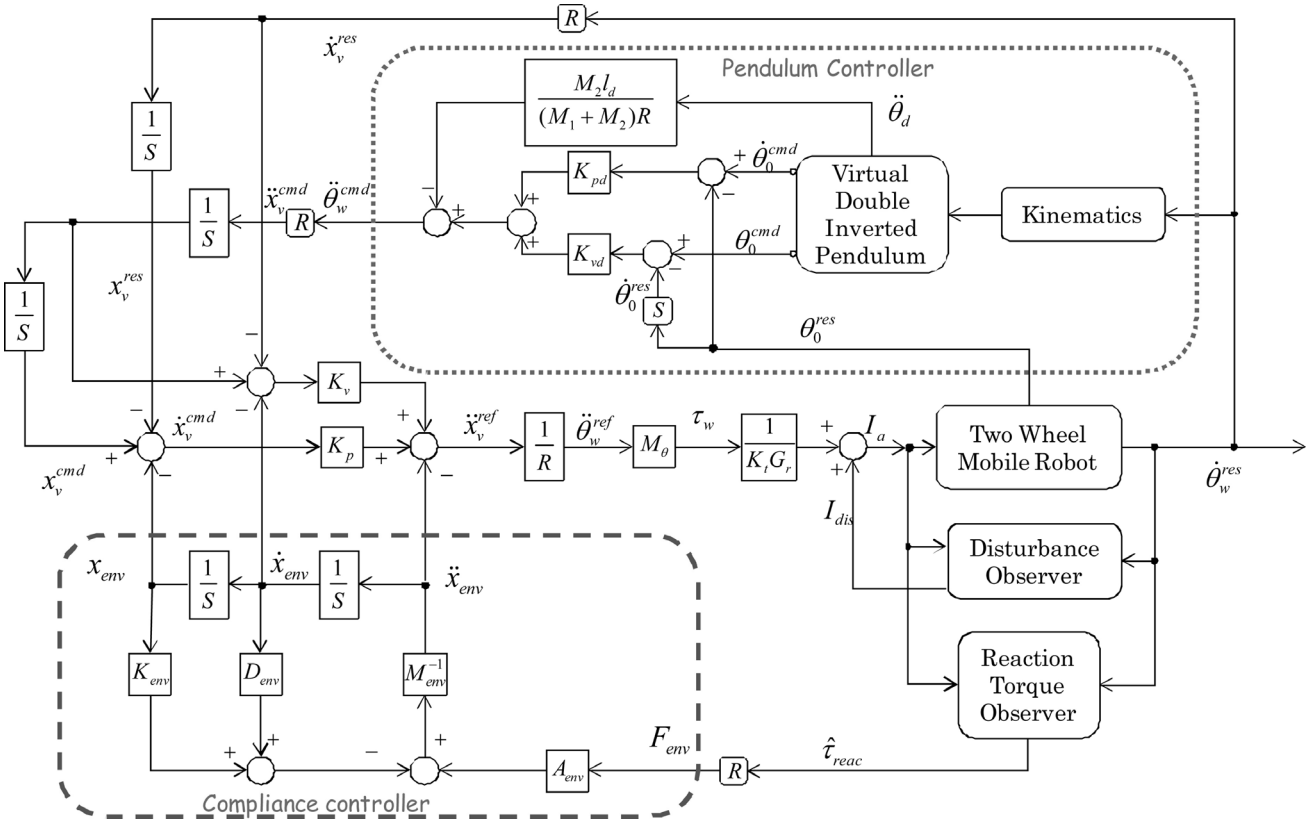

Fig. 5. Wheel controller with compliance control.

$q = (\theta_0 , \theta_1 , \theta_2 , \theta_3)$ and x is the position vector in workspace.

$$x = f(q) \tag{28}$$

$$\dot{x} = J_{aco}(q)\dot{q} \tag{29}$$

$$\ddot{x} = J_{aco}(q)\ddot{q} + \dot{J}_{aco}(q)\dot{q} \tag{30}$$

where $J(q)$ is Jacobean matrix. Position vector in workspace, x becomes COG positions of virtual inverted pendulum. Therefore kinematics represented by $f(q)$ is explained by (31).

$$f(q) = \begin{bmatrix} m_1 l_0 S_0 + m_2 l_1 S_{01} + m_3 l_2 S_{012} + m_4 l_3 S_{0123} \\ m_1 l_0 C_0 + m_2 l_1 C_{01} + m_3 l_2 C_{012} + m_4 l_3 C_{0123} \end{bmatrix} \tag{31}$$

Abbreviations are defined in (7). In the redundant manipulator, joint space acceleration reference, $\ddot{q}^{ref}$ which was obtained using pseudo inverse matrix, can be written as (32). In (32), the first term is the workspace acceleration and the second term represents the null space motion.

$$\ddot{q}^{ref} = J^{+}(\ddot{x}^{ref} - \dot{J}\dot{q}) + (I - J^{+}J)\ddot{\phi} \tag{32}$$

where, J^{+} is the weighted pseudo inverse matrix and defined as (33).

$$J^{+} = W^{-1}(J^{T} J\, W^{-1} J^{T})^{-1} \tag{33}$$

W of the above equation is a diagonal weighting matrix. In the joint space a disturbance observer based acceleration controller, W corresponds with the virtual inertia matrix I_{vn} and can be selected arbitrary [22]. By using the joint space and workspace observers in (32), it can be rewritten as (34) without calculating the $\dot{J}(q)\dot{q}$ and $(I - J^{+}J)$ terms [23].

$$\ddot{q}^{ref} = J^{+}\ddot{x}^{ref} + \ddot{q}^{ref}_{null} \tag{34}$$

The workspace acceleration reference $\ddot{x}^{ref}$ is given in (35).

$$\ddot{x}^{ref} = K_{hp}(x^{cmd} - x\ ) + K_{hp}(\dot{x}^{cmd} - \dot{x}\ ) \tag{35}$$

where, K_{hp} and K_{hv} are the proportional gain and derivative gain respectively. x is the COG position vector in the workspace of the inverted pendulum and x_{cmd} is the COG position vector in the workspace of the inverted pendulum.

Null space acceleration reference, $\ddot{q}^{ref}_{null}$ is calculated as shown in (36). $\dot{q}^{cmd}$ and $\dot{q}^{res}$ are angular position command and angular position response respectively.

$$\ddot{q}^{ref}_{null} = k_v(\dot{q}^{cmd} - \dot{q}^{res}) \tag{36}$$

Fig. 6 shows the detailed block diagram of the posture control of the manipulator.

The angular acceleration reference ($\ddot{q}^{ref}$) was calculated as shown in (34). Motor inertias were used to derive the input torques of the manipulator motors. Position responses of all links were used to model the virtual inverted pendulum. In addition to this, position and velocity responses were used to calculate the feedback signals to the workspace. Disturbance observers were implemented to each and every motor.

A workspace observer was constructed to compensate the workspace error and Fig. 7 illustrates a diagram of it.

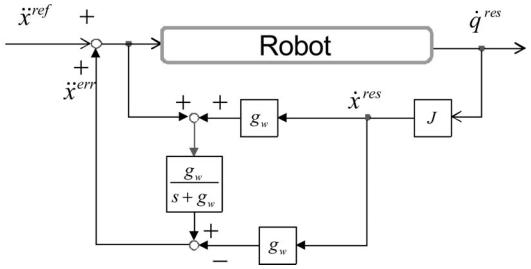

Fig. 7. Block Diagram of workspace observer.

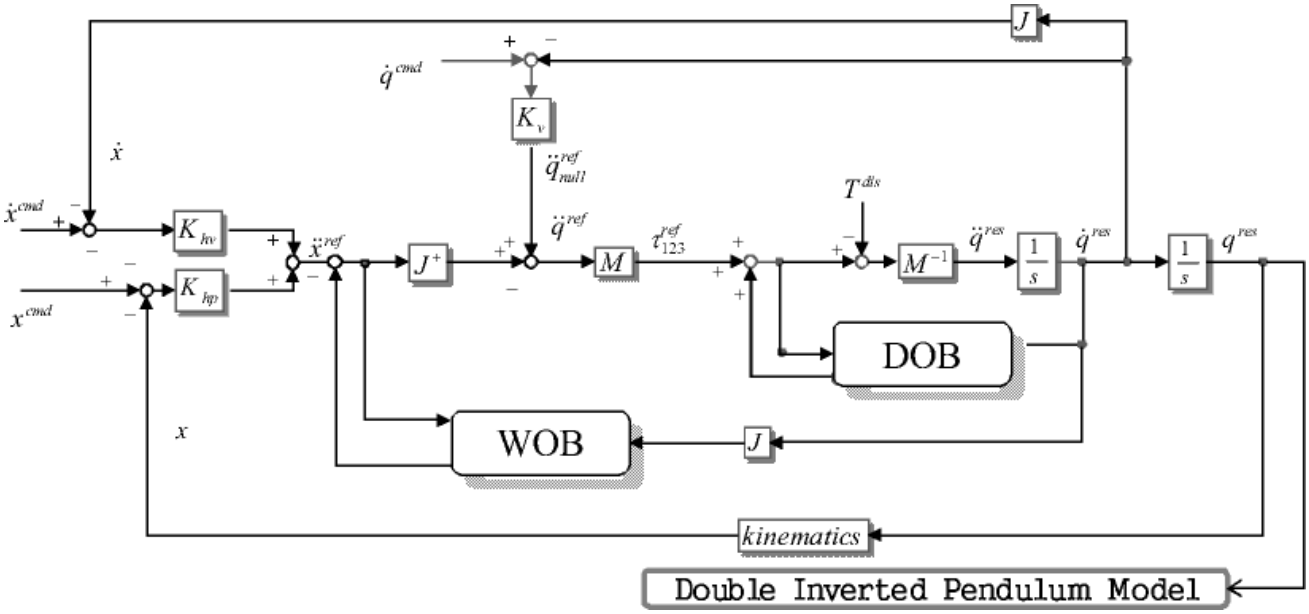

Fig. 6. Block diagram of manipulator control.

Reference acceleration and velocity in the workspace are the inputs to the workspace observer and g_w is the workspace gain. $\ddot{x}^{ref}$ is the acceleration reference of the position vector and $\ddot{x}^{err}$ is the acceleration error of the position vector. $\dot{x}^{res}$ and $\dot{q}^{res}$ are linear velocity response and angular velocity response respectively.

5. Disturbance observer, reaction torque observer and compliance control

A. Disturbance Observer

Disturbance observers were implemented on the motor controllers to cancel the disturbance effects [21]. This section describes the architecture and characteristics of a disturbance observer. When a servomotor with one degree of motion is considered, under an ideal motor driver, a servomotor in the joint space can be represented as (37),

$$M\ddot{q} = \tau_m - \tau_l \tag{37}$$

Where,
τ_m Generated torque of the motor,
τ_l Load torque,
M Motor inertia,
$\ddot{q}$ Angular acceleration.

The total generated torque can be expressed as

$$\tau_m = K_t I_a = K_t I_a^{ref} \tag{38}$$

K_t is a function of flux position and expanded in Fourier series and is called a torque coefficient. I_a is torque current. In most cases, it is possible to regard I_a as torque current reference I_a^{ref}.

$$\tau_l = \tau_{\text{int}} + \tau_{ext} + F + D\dot{q} \tag{39}$$

Where, τ_{int} is the interactive torque including the Coriolis term, the centrifugal term and gravity term. τ_{ext} is the reaction torque when the mechanical system does the force task. F and $D\dot{q}$ are Coulomb and viscous friction, respectively. Substituting (38) and (39) into (37) yields (40).

$$M\ddot{q} = K_t I_a - (\tau_{\text{int}} + \tau_{ext} + F + D\dot{q}) \tag{40}$$

The parameters in (40) are the inertia and the torque coefficient. The inertia will change according to the mechanical configuration of the motion system.

$$M = M_n + \Delta M \tag{41}$$

The torque coefficient will vary according to the rotor position of the electric motor due to irregular distribution of magnetic flux on the surface of rotor.

$$K_t = K_{tn} + \Delta K_t \tag{42}$$

Total disturbance torque τ_{dis} can be defined as follows.

$$\tau_{dis} = \tau_l + \Delta M\ddot{q} - \Delta K_t I_a^{ref} = \tau_{\text{int}} + \tau_{ext} + \\ + F + D\dot{\theta} + (M - M_n)\ddot{\theta} + (K_t - K_{tn})I_a \tag{43}$$

K_{tn} and M_n are the nominal torque coefficient and the inertia, respectively. ΔK_t and ΔM are torque coefficient fluctuation and inertia fluctuation respectively. However, dynamic equation yields,

$$(M_n + \Delta M)\ddot{q} = (K_{tn} + \Delta K_t)I_a - \tau_l \tag{44}$$

Rearranging (44), equation (45) can be obtained. Therefore disturbance torque can be obtained as (46).

$$M_n\ddot{q} - K_{tn}I_a = -(\tau_l + \Delta M\ddot{q} - \Delta K_t I)_a \tag{45}$$

$$\tau_{dis} = K_{tn}I_a - M_n\ddot{q} \tag{46}$$

It is hard to implement an ideal differentiator. Therefore, a pseudo-differentiator is used to obtain the acceleration. In addition, noise is included in velocity signal. Low pass filler is inserted to reduce the effect of this noise. Total calculation process of the disturbance can be represented as shown in (47). Fig. 8 depicts the disturbance observer. g_{ob} is the disturbance observer gain.

$$\hat{\tau}_{dis} = \frac{g_{ob}}{s + g_{ob}}\left(K_{tn}I_a + g_{ob}M_n\dot{\theta}\right) - g_{ob}M_n\dot{\theta} \tag{47}$$

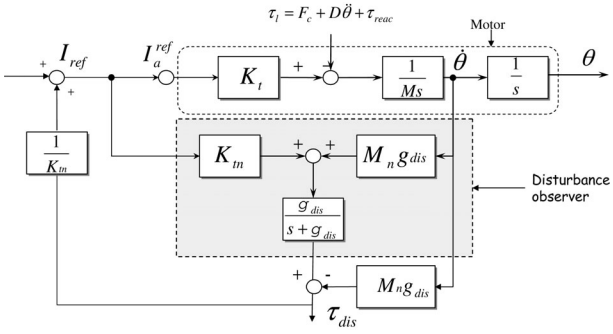

Fig. 8. Block diagram of disturbance observer.

B. Reaction Torque Observer

The disturbance torque estimated by (47) in the previous section, is used for a realization of robust motion control. It is effective not only for the disturbance compensation but also the parameter identification in the mechanical system. The output of the disturbance observer is only the friction effect under the constant angular velocity motion. This feature makes it possible to identify the friction effect in the mechanical system. The external force effect is also identified by using the estimated disturbance [12]. Here, it is assumed that the friction effects are known beforehand by the above identification process. By implementing the angular accelerated motion the system parameters are adjusted in the observer design so that they are close to the actual values. As a result, τ_{reac} can be calculated as in (48).

$$\tau_{reac} = \tau_{dis} - \tau_{\text{int}} - F - D\dot{\theta} - (M - M_n)\ddot{\theta} - \\ - (K_t - K_{tn})I_a \tag{48}$$

τ_{reac} Reaction torque,
τ_{int} Interactive torque,
F Coulomb friction,
$D\dot{\theta}$ Viscous friction,
M_n Nominal value of motor inertia,
K_{tn} Nominal value of current coefficient,
$\hat{\tau}_{reac}$ Estimated reaction torque.

Here, it is assumed that the nominal values of Mn and Ktn have been finely adjusted such that it is almost equal to the actual values. Total calculation process of reaction torque observer is shown in (49).

$$\hat{\tau}_{reac} = \frac{g_{reac}}{s + g_{reac}}\left(K_{tn} I_a + g_{reac} M_n \dot{\theta} - \right. \\ \left. - \tau_{\text{int}} - F - D\dot{\theta}\right) - g_{reac} M_n \dot{\theta} \tag{49}$$

Fig. (9) depicts the reaction torque observer.

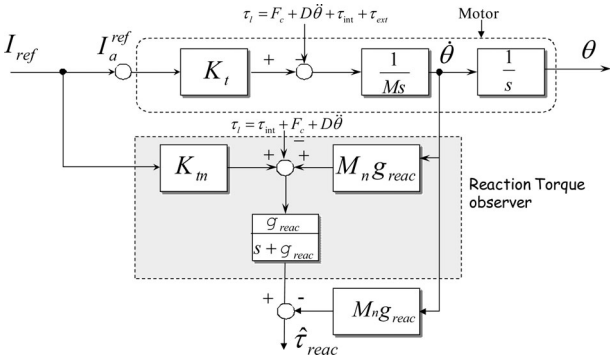

Fig. 9. Block diagram of reaction torque observer.

C. Compliance Control

The compliance control is the control system of compensating trajectory so that external force may be followed, when force is received from the external world. It is possible to realize stable contact with the environment by this, and it becomes possible to give the robot flexibility [19],[20]. Virtual impedance characteristics are set as a mass damper-spring model. If the virtual impedance characteristics are M_C, D_C, K_C and force feedback gain is A_C, Equation (50) explains the conversion of force command into position command, x_C . $\ddot{x}_C$ and $\dot{x}_C$ are acceleration command and velocity command of the compliance controller.

$$M_C \ddot{x}_C + D_C \dot{x}_C + K_C x_C = A_C F_C \tag{50}$$

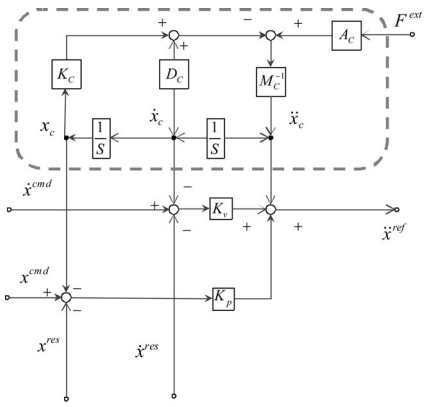

Fig. 10. Block diagram of compliance control.

The compliance control based position control system is implemented by applying disturbance observer. Equation (51) and Fig. 10 is explained compliance control based position control system.

$$\ddot{x}^{ref} = K_p (x^{cmd} - x^{res} - x_C) + \\ + K_v (\dot{x}^{cmd} - \dot{x}^{res} - \dot{x}_C) - \ddot{x}_C \tag{51}$$

6. Validation of proposed method

In order to verify the proposed method simulation and experiment was conducted. First, we explain the simulation method and its result. Then experiment and results are described.

A. Simulation

Simulation was carried out to check the validity of proposed method. Spring-damping model used to model the environment [26]. Environment was modeled by using spring damper model and modeling is explained by (52). K_e and D_e are damping coefficient and viscous damper of damping model, respectively.

$$F_{ext} = K_e \Delta x + D_e \Delta \dot{x} \qquad (if \quad \Delta x \le 0)$$
$$F_{ext} = 0 \qquad (otherwise) \tag{52}$$

$$\Delta x = x_{env} - x^{ref} \qquad x^{ref} = \int \dot{x}^{ref} dt \qquad \dot{x}^{ref} = \int \ddot{x}^{ref} \tag{53}$$

OpenGL simulation set up was used and it is shown in Fig. 11. Simulation parameters are given in table (V).

Table 5. Simulation parameter.

Symbol	Value	Symbol	Value
K_e	6000.0	D_e	600.0
ω_{env}	10.0	ζ_{env}	1.0
C_{env}	0.0001		

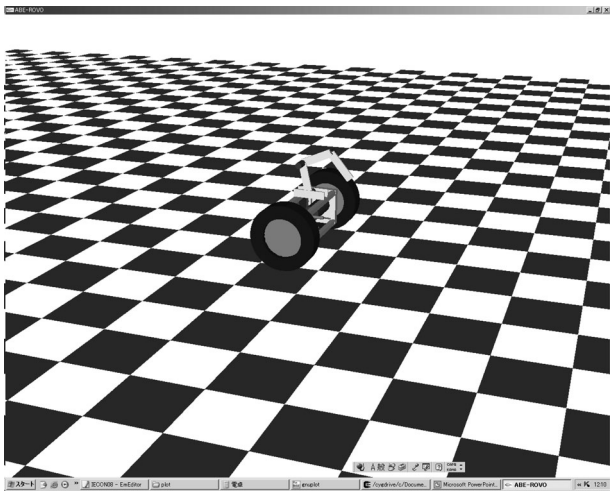

Fig. 11. Simulation setup.

In simulation, we injected the force to the wheel controller during 4.5 seconds and 5 seconds. Physical meaning of this is, wheel collides an object on the floor after 4.5 seconds and goes over that objects for 0.5 seconds.

Then we observed the resultant torque from the damping model and proposed reaction torque observer and results are shown in Fig. 12. Fig. 13 clarifies that there is a torque riffle when colliding and releasing an object. Variation of passive joint angle is shown in Fig. 14 and variation of COG positions are shown in Fig. 15 and Fig. 16. Simulation results are proved that the proposed controller is strong enough to stabilize the system quickly.

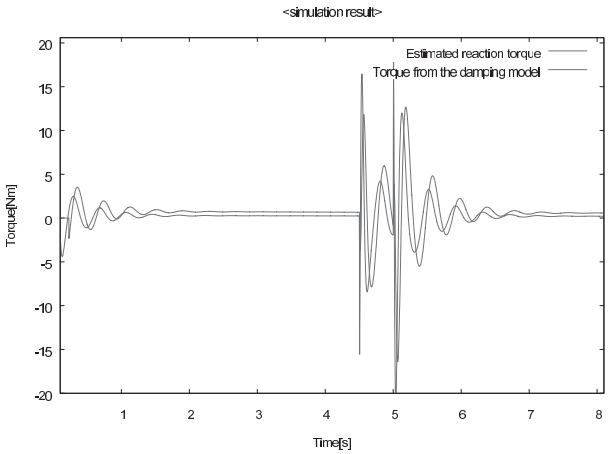

Fig. 12. Torques from the environment.

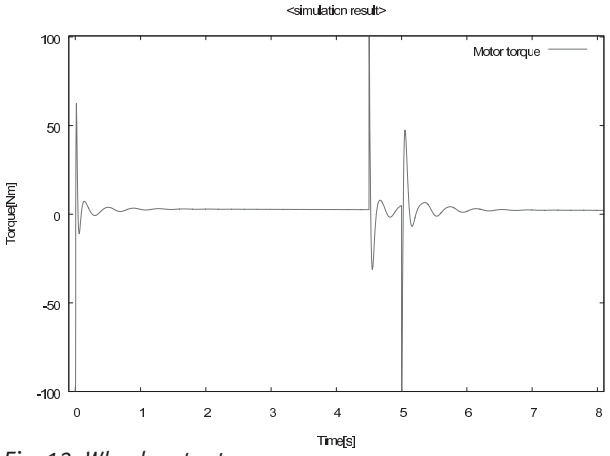

Fig. 13. Wheel motor torque.

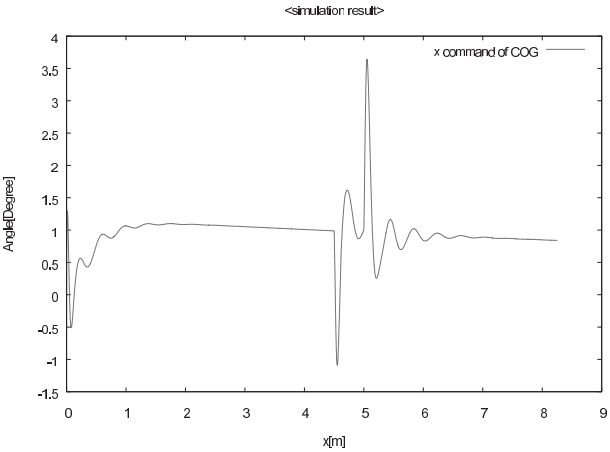

Fig. 14. Angle of passive joint.

B. Experiment

An experiment was conducted to check the validity of the proposed method using the two-wheel mobile manipulator, which is shown in Fig. 1. Before the experiment itself, a constant velocity test was carried out to estimate the reaction torque. Reaction torque was estimated by utilizing disturbance torque, which is measured through the disturbance observer. According to the definition, terms of gravity and friction effect should be removed from disturbance torque to calculate the reaction torque. By performing several constant velocity tests, the gravity and friction effect can be estimated [12]. Therefore, a constant velocity test was carried out for the wheel motors. Equation (54) shows the equation of friction effect. In this case the gravity effect is relatively small.

$$\left.\begin{aligned} \dot{q}\langle 0.0, \quad F + D\dot{q} = 0.96 - 13.6\dot{q} \\ \dot{q}\rangle 0.0, \quad F + D\dot{q} = 0.96 - 13.6\dot{q} \end{aligned}\right\} \tag{54}$$

Thereafter, the experiment was carried out in an environment with an irregular floor. Since the laboratory floor is a smooth surface, it was made rough by laying floor carpets as shown in Fig. 17.

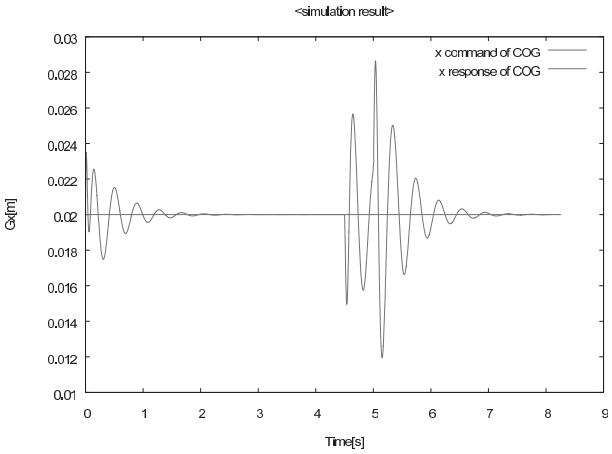

Fig. 15. X position of the pendulum.

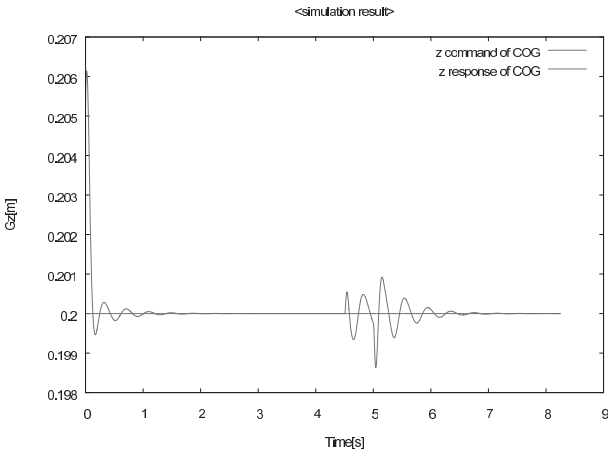

Fig. 16. Z position of the pendulum.

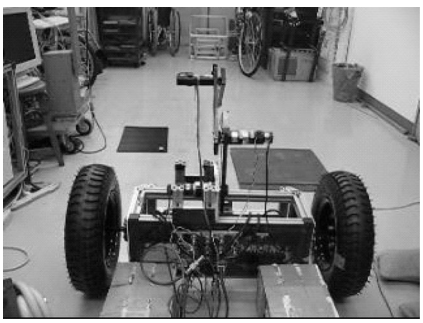

Fig. 17. Experiment set up.

Initially the robot was moved on a straight-line trajectory without the proposed environmental interaction method. It failed to deal with this successfully. Thereafter, the proposed compliance control based PD controller was applied to the robot wheels and the experiment was repeated for same trajectory. The robot moved successfully over the rough floor this time and the data was collected. Robot details are shown in Table 6 and experimental parameters are given in Table 7 with the descriptions.

Table 6. Robot parameter used in experiment.

Description	Mass kg	Description	Length m
Mass of a wheel	8.5	Radius	0.2
Mass of the body	13.0	Length of the link 0	0.125
Mass of the link 1	1.06	Length of the link 1	0.2
Mass of the link 2	0.84	Length of the link 2	0.2
Mass of the link 3	0.5	Length of the link 3	0.18

Table 7. Experimental parameter.

Symbol	Value	Symbol	Value	Symbol	Value
K_p	900.0	K_v	60.0	K_{hp}	900.0
K_{hv}	60.0	K_{pd}	10.5	K_{vd}	27.2
g_{ob}	30.0	g_w	60.0	g_{reac}	30.0
ω_{env}	5.0	ζ_{env}	1.0	C_{env}	0.00005

In our experimental work without the proposed method only the conventional PD control was used for wheel control. Then we applied the controller modified using compliance control. The two-wheel mobile manipulator is a self-balancing robot, which does not have any supportive wheels or castors. Therefore it is likely to become unstable even when submitted to small disturbances from the environment. Therefore we used two floor carpets, which were not very thick. With only conventional PD control, the robot failed to get over the carpets. However with the modified controller the experiment succeeded and the robot was able to move over carpets.

The inclination angle of the body is depicted by Fig. 18. When the robot passed over the step on the floor, the inclination angle increased slightly. However, after passing the barrier, our proposed controller reduced the inclination angle variation back to its normal.

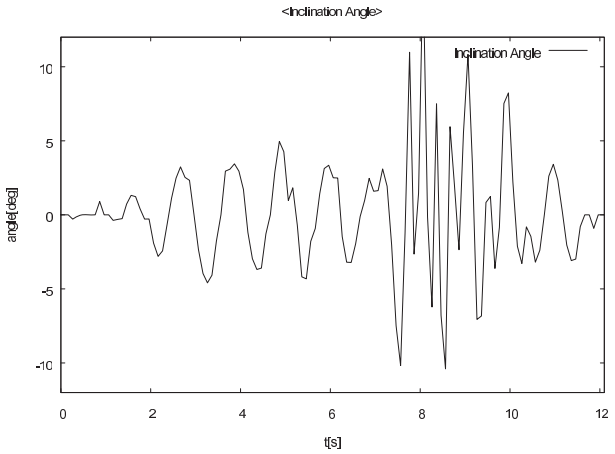

Fig. 18. Inclination angle (passive joint).

Fig. 19 depicts torque variation of the wheel motor. It is clear that torque has been increased at the barriers. However, the controller was strong enough to stabilize the motor torque. Fig. 20 shows the position variation of the two-wheel mobile robot over time. Until body balance was achieved, the robot did not move forward. After achieving the balancing of the body, the robot started to move forward. While moving, it went over the carpets that had been laid.

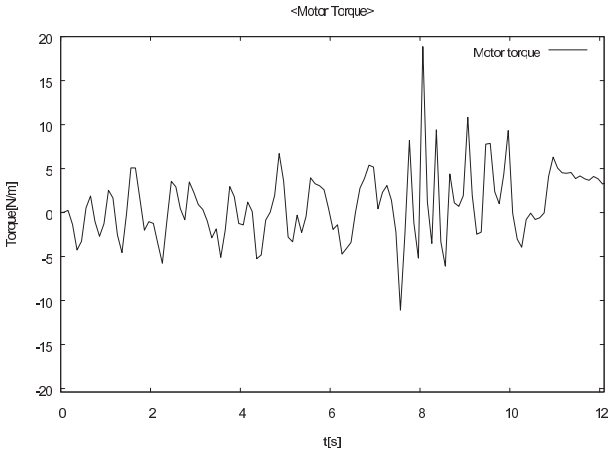

Fig. 19. Reaction torque from environment.

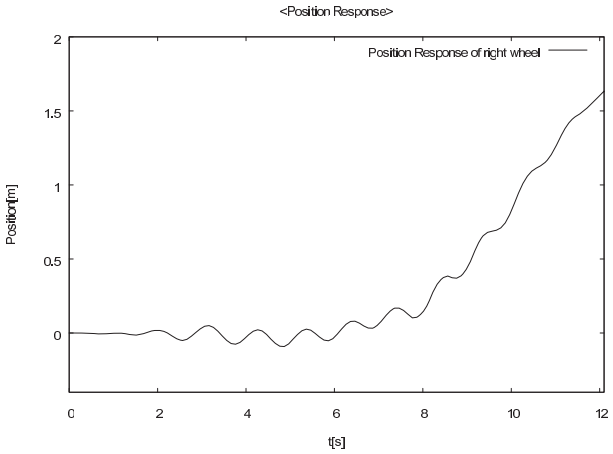

Fig. 20. Position response of robot.

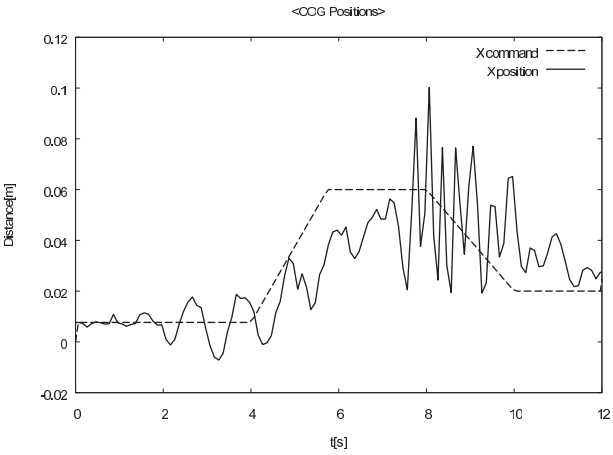

Fig. 21. x position of COG.

Fig. 21 and Fig. 22 illustrate the COG positions of the virtual inverted pendulum. Dot lines are the command values in both cases. COG response shows a small amount of variation when going over the floor barrier. However, it

becomes stable very quickly and this proves the effectiveness of the proposed controller.

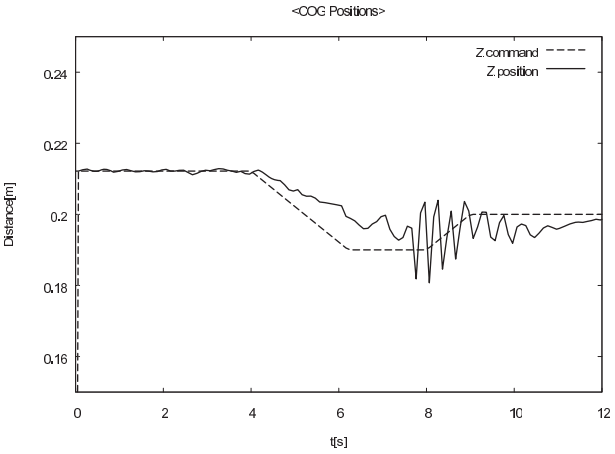

Fig. 22. z position of COG.

7. Conclusion

In this paper, a robust wheel controller for rough terrain has been proposed using a reaction torque observer. The two-wheeled mobile manipulator should be stable in the face of external disturbance coming from the environment. A control system, which can handle the environmental disturbances, was developed using reaction torque feedback and compliance control. First, simulation was implemented to check the validity of proposed method. Then, an experiment was conducted to check the validity of the proposed method. In the experiment, with the proposed method the mobile manipulator could run over the barriers, which were laid, on the floor. Without the proposed method, the system became unstable when confronted with the barrier. Therefore the effectiveness of the proposed method is justified.

AUTHORS
Pradeep Kumara W. Abeygunawardhana, Toshiyuki Murakami* - Keyo University, Yokohama, Japan. E-mail: abeygunawardhana@yahoo.com
* Corresponding author

References

[1] Ch.-I., Fu L.-Ch., "Passivity based control of the double inverted pendulum driven by a linear induction motor". In: *Proceedings of 2003 IEEE Conference on Control Applications (CCA) 2003*, 23rd-25th June 2003, vol. 2, pp. 797-802.

[2] Yasunobu S., Iwasaki T., "Swing up intelligent control of double inverted pendulum based on human knowledge". In: *SICE 2004 Annual Conference*, 4th-6th August 2004, vol. 2, pp. 1869-1873.

[3] Grasser F., Aldo D'Arrigo, Silvio Colombi, "JOE: A Mobile, Inverted Pendulum", *IEEE Transactions on industrial electronics*, vol. 49, no. 1, 2002.

[4] Hiroshi N., Murakami T., "An Approach to self Stabilization of Bicycle Motion by Handle Controller". In: *Proceedings of the First Asia International Symposium on Mechatronics*, September 2004.

[5] Iuchi K., Hiroshi N., Murakami T., "Attitude Control of Bicycle Motion by Steering Angle and Variable COG Control". In: *IECON 2006. 32nd Annual Conference of IEEE Industrial Electronics Society*, 6th-10th Nov. 2006, pp. 2065-2070.

[6] Abe H., Shibata T., Murakami T., "A Realization of Stable Attitude Control of two-wheels Driven Mobile Manipulator". In: *IEEE AISM Conference*, December 2006.

[7] Shibata T., Murakami T., "A Null Space Control of two-wheels Driven Mobile Manipulator Using Passivity Theory". In: *Second Asia International Symposium on Mechatronics (AISM 2006)*.

[8] Abeygunawardhana P.K.W., Murakami T., "Industrial Electronics Society, 2007. IECON 2007. 33nd Annual Conference of IEEE". In: *Second Asia International Symposium on Mechatronics (AISM 2006)*, 5th-8th Nov. 2007, Taipei, Taiwan, pp. 2712-2717.

[9] Miyashita T., Ishiguro H., "Behavior Selection and Environment Recognition Methods for Humanoids based on Sensor History". In: *Proceedings of the 2006 IEEE/RSJ International Conference on Intelligent Robots and Systems*, 9th–15th October 2006, Beijing, China, pp. 3468-3473.

[10] Perez-Mendoza S.J., Ayala-Ramirez V., "Visual servoing for micro robotic platforms". In: *Proceedings of the 14th International Conference on Electronics, Communications and Computers (CONIELECOMP'04)*, 16th-18th Feb. 2004, pp. 18 – 22.

[11] Zha H., Tanaka K., Hasegawa T., "Detecting Changes in a Dynamic Environment for Updating its Maps by Using a Mobile Robot". In: *IROS'97. Proceedings of the IEEE/RSJ International Conference on Intelligent Robots and Systems*, 7th-11th Sept. 1997, vol. 3, pp. 1729-1734.

[12] Murakami T., Yu F., Ohnishi K., "Torque Sensorless Control in Multi degree of Freedom Manipulator", *IEEE Transaction on Industrial Electronics*, vol. 40, no. 2, April 1993, pp. 259-265.

[13] Kim J.-O., Khosla P. K., "Real-time obstacle avoidance using harmonic potential functions", *IEEE Transactions on Robotics and Automation*, vol. 8, issue 3, June 1992, pp. 338-349.

[14] Rimon E., Koditschek D. E., "Exact robot navigation using artificial potential functions", *IEEE Transactions on Robotics and Automation*, vol. 8, issue 5, October 1992, pp. 501-518.

[15] Utkin V.I., Drakunov S.V., Hashimoto H., Harashima F., "Robot path obstacle avoidance control via sliding mode approach". In: *Proceedings IROS. IEEE/RSJ International Workshop on Intelligent Robots and Systems Intelligence for Mechanical Systems*, 3rd-5th November 1991, vol. 3, pp. 1287-1290 .

[16] Choi J.-S., k Kim B.-K., "Near-time-optimal trajectory planning for wheeled mobile robots with translational and rotational sections", *IEEE Transactions on Robotics and Automation*, vol. 17, issue 1, February 2001, pp. 85- 90.

[17] Fujimura K., "Route Planning For Mobile Robots Amidst Moving Obstacles". In: *Proceedings of the 1992 EEE/RSJ International Conference on Intelligent Robots and Systems*, 7th-10th July 1992, vol. 1, pp. 433-438.

[18] Nagami A., Murakami T., Ohnishi K., "A power-assistant platform taking environmental disturbance into ac-

count". In: *Proceedings of the 6th International Workshop on Advanced Motion Control*, 2000, pp. 152-157.

[19] Katsura S., Ohnishi K., "Human Interaction by a Wheelchair". In: *IECON'02. Industrial Electronics Society, IEEE 28th Annual Conference*, vol., 5th-8th Nov. 2002, pp. 2758-2763.

[20] Katsura S., Ohnishi K., "A Wheelchair type mobile robot Taking Environment Disturbance into Account", In: *7th International Workshop on Advanced Motion Control*, 3rd-5th July 2002, pp. 500-505.

[21] Kouhei O., Murakami T., Masaaki S., "Motion control for Advanced Mechatronics", *IEEE/ASME Transactions on Mechatronics*, vol. 1, no. 1, March 1996, pp. 56-67.

[22] Oda N., Murakami T., Ohnishi K., "A force based motion control strategy for hyper-redundant manipulator". In: *IECON'97. 23rd International Conference on Industrial Electronics, Control and Instrumentation*, 9th-14th Nov. 1997, vol. 3, pp. 1385-1390.

[23] Murakami T., Kahlen K., De Doncker R.W.A.A., "Robust motion control based on projection plane in redundant manipulator", *IEEE Transactions on Industrial Electronics*, vol. 49, issue 1, February. 2002, pp. 248-225.

[24] Abeygunawardhana P.K.W., Murakami T., "Environmental Interaction of two-wheel Mobile Manipulator using Reaction Torque Observer". In: *Proceedings of the 2008 IEEE International Conference on Advance Motion Control. AMC'08*, 26th – 28th March 2008.

[25] Huang Q., Chen X.D., Oka K., "Phased Compliance Control with Virtual Force for Six Legged Robot", *International Journal of Innovative Computing Information and Control*, vol. 4, issue: 12, December 2008, pp. 3359-3373.

[26] Morisawa M., Kouhei O., "*Parallel Link Biped Robot Motion Control*", PhD Dissertation, 2003, pp. 45-46.